

Plasma production for the 50 MeV plasma lens experiment at LBL*

W. Leemans, B. van der Geer, M. de Loos, M. Conde, R. Govil and S. Chattopadhyay
Lawrence Berkeley Laboratory
1 Cyclotron Road, Berkeley, CA 94720 USA

Abstract

The Center for Beam Physics at LBL has constructed a Beam Test Facility (BTF) housing a 50 MeV electron beam transport line, which uses the linac injector from the Advanced Light Source, and a terawatt Ti:Al₂O₃ laser system. The linac operates at 50 MeV and generates 15 ps long electron bunches containing a charge of up to 2 nC. The measured unnormalized beam emittance is 0.33 mm-mrad. These parameters allow for a comprehensive study of focusing of relativistic electron beams with plasma columns, in both the overdense and underdense regime (adiabatic and tapered lenses). A study of adiabatic and/or tapered lenses requires careful control of plasma density and scale lengths of the plasma. We present experimental results on the production of plasmas through resonant two-photon ionization, with parameters relevant to an upcoming plasma lens experiment.

I. INTRODUCTION

Plasma lenses [1] are of two types: overdense and underdense. In an overdense lens the beam density n_b is a small perturbation to the plasma density n_p . The plasma dynamics can therefore be described by linear theory. The focusing gradient however is non-linear due to its dependence on the electron beam density. In an underdense lens ($n_b > n_p/2$), the plasma dynamics become highly non-linear. The focusing gradient for this case however is linear since it depends on the plasma density. One example of an underdense lens is the tapered lens [2] in which the ratio between plasma and beam density is maintained constant. In addition, a so called adiabatic lens has been proposed as a way of focusing electron beams to spot sizes shorter than the Oide limit.[3]

There are two requirements which must be satisfied to enhance the efficacy of the lenses. They are (a) that the plasma response time must be short compared to the pulse length, i.e. $\omega_p \sigma_\tau > 1$, and (b) that the plasma return currents within the beam must be small. Here σ_τ is the rms electron bunch duration and ω_p is the plasma frequency.

Previous observation of plasma lens behavior in the overdense regime has been made at the Argonne National Laboratory, at KEK and most recently at UCLA.[4-6] Only the UCLA experiment showed clear beam size reduction and the effect of temporal lens dynamics.

To this date no experiments have been reported showing focusing of electron beams by plasma lenses operating in the underdense regime, nor has there been a systematic study of return currents, adiabatic lenses, etc.

Aside from having the potential to enhance luminosity in future linear colliders, plasma lenses could be useful as small

f-number lenses to tightly focus relativistic beams of moderate energy.

II. PLASMA LENS EXPERIMENT

A. The Beam Test Facility

The scope of the plasma lens experiment at LBL is to study the properties of plasma lenses in both overdense and underdense regimes. Emphasis will be on resolving important issues such as time response of the lens, lens aberrations and shot-to-shot reproducibility. Experiments are planned using the 50 MeV electron beam at the Beam Test Facility (BTF) at LBL.

The BTF, operated under the auspices of the Center for Beam Physics in support of its experimental R&D program, has recently been constructed. The details of the design of the transport line have been reported previously [7]. The commissioning phase of the line is nearing completion. The main linac parameters are given in Table 1.

Table 1: ALS Linac parameters

| | |
|-----------------------------------|------------------|
| Maximum Energy | 50 MeV |
| Charge | 1-2 nC/bunch |
| Bunch Length (σ_z) | 10-15 ps |
| Emittance rms (unnorm.) | 0.3 mm-mrad |
| # bunches/macropulse @ 125 MHz | 1 - 10 (max 100) |
| Macropulse rep. rate | 1 - 10 Hz |

The line has been designed to allow a variety of experiments to be carried out. A wide range of diagnostics have been built and implemented to allow full characterization of the electron beam. These include integrating current transformers for charge measurement, high bandwidth beam position monitors, fluorescent screens for transverse beam analysis and an optical transition radiation (OTR) diagnostic system [8]. The OTR system allows for single bunch measurement of beam emittance, energy, charge and bunch length. Two quadrupole triplets upstream of the plasma lens chamber will allow good control over the transverse properties of the electron beam at the entrance of the plasma lens (β ranging from 0.02 to 0.4 m).

B. Plasma lens model

Using an envelope model, we have determined the plasma requirements (density, length and location) and the beam requirements (waist size, location, charge) which will allow us to study the different regimes.

The design calculations have been carried out using the following envelope model for the beta function β [9]:

$$\frac{d^3\beta}{ds^3} + 4K \frac{d\beta}{ds} + 2\beta \frac{dK}{ds} = 0. \quad (1)$$

* This work was supported by the Director, Office of Energy Research, Office of High Energy and Nuclear Physics, High Energy Physics Division, of the U.S. Department of Energy under Contract No. DE-AC03-76SF00098.

Here K is the plasma lens strength given by $K = 2\pi r_e n_p / \gamma$ or $K = 2\pi r_e n_b / \gamma$ depending upon whether the plasma is underdense ($n_p < 2 n_b$) or overdense ($n_p > 2 n_b$), r_e is the classical electron radius, γ is the Lorentz factor and s is the longitudinal coordinate. The boundary conditions on the envelope equation are that β and β' be continuous, and that β'' jump by $-2K\beta$ at a discontinuity in K . Due to focusing of the plasma lens the beam size will change and, therefore, in the overdense case the focusing will change. This effect must be taken into account. In terms of the quantity β we can write: $n = (\beta_o / \beta) n_{bo}$, where β_o and n_{bo} are the initial beta function value and beam density at the entrance to the plasma lens respectively. Plasma return currents reduce the effect of the lens.[10] The effect is approximately given by:

$$K_{rc} = \frac{K_{arc}}{1 + (k_p a_b)^2}, \quad (2)$$

where k_p is the plasma wavenumber (ω_p/c), a_b is the beam radius and K_{arc} and K_{rc} are the K -value without and with return current effect included.

We have integrated the β -equation numerically considering a variety of plasma lengths and position of such lenses. Using this model we have determined that plasma lengths on the order of 10 to 50 cm and densities in the range of $5 \times 10^{12} \text{ cm}^{-3}$ to $2 \times 10^{14} \text{ cm}^{-3}$ should allow a comprehensive study of overdense plasma lenses at the BTF, including a study of time response effects, aberrations and return currents. The requirements on the electron beam and on the plasmas are more restrictive for an adiabatic lens. Assuming that the plasma profile is given by

$$n_p(s) = \frac{1 + (\beta_o' / 2)^2}{K_1 (\beta_o + \beta_o' s)^2}, \quad (3)$$

and requiring the beam density $n_b(s)$ to be larger than the plasma density, leads to the following inequality:

$$\frac{4N_b r_e \beta_o}{\sqrt{2\pi\sigma_z \epsilon_n}} - 4 > (\beta_o')^2. \quad (4)$$

Here N_b is the number of beam particles, ϵ_n is the normalized emittance, $K_1 = 2\pi r_e / \gamma$, and β_o and β_o' are the beta-function and its derivative at the lens entrance. The criterion becomes easiest to satisfy at a focus ($\beta_o' = 0$). Using the relation between β_o' and β_o appropriate to a drift region, one obtains

$$\beta_{o\min}^* (\text{cm}) = \frac{641 \epsilon_n (\text{cm-rad})}{Q_b (\text{nC})}. \quad (5)$$

If, in addition, the plasma response time must be adequately short ($k_p \sigma_z > 2$) then $Q_b (\text{nC}) > 204 \epsilon_n (\text{cm-rad})$. Plasmas with lengths up to 10 cm and densities changing from 10^{14} to 10^{16} cm^{-3} over that distance will be required.

C. Plasma lens design

We have chosen to produce plasmas through two-photon ionization of tri-propylamine (TPA) using a UV-laser. TPA has a large ionization cross section [11] and high vapor pressure (3.5 Torr). The plasmas produced with this method are field free and do not require any magnetic confinement.

The plasma density as a function of neutral gas density N_o [cm^{-3}] and laser intensity I [W/cm^2] is given by

$$n_p = \frac{N_o \alpha I^2 \Delta t}{h\nu}. \quad (6)$$

Here Δt is the HWHM of laser pulse [s], $h\nu$ the photon energy [J] and α the two-photon ionization coefficient [cm^4/W]. The scaling law suggests two ways of creating plasmas with longitudinally varying plasma densities: using a pressure gradient (e.g. differential pumping) or changing the laser intensity as a function of distance along the electron beam. Because of its simplicity we are opting at present for the second approach.

The plasma chamber is isolated from the electron beam transport line by a 3 μm beryllium window. The laser beam enters the vacuum chamber through an AR coated window, and is made to propagate colinearly with the electron beam axis using an ultra-thin UV mirror ($R = 90\%$), made out of 5 μm nitrocellulose substrate. The effect such a substrate and the Be-foil have on beam emittance is presently being studied. The plasma length can be controlled by adjusting the spacing between this mirror and a second mirror which deflects the laser beam.

Spatially and temporally resolved transverse electron beam dynamics will be measured using OTR. An aluminized foil mounted on a retractable shaft will allow measurement of the electron beam profile over at least five "Rayleigh ranges".

We next discuss preliminary results on the generation of plasmas through two-photon ionization. The main emphasis of this study was to verify the density scaling law. The experiment at the BTF will utilize a frequency quadrupled Nd:YAG laser at 266 nm which produces about 200 mJ in a 7 ns long pulse. No significant differences are expected with the results at 248 nm [12].

D. Plasma production through two-photon ionization

The experimental lay-out is shown in Fig. 1. Plasma is produced by a KrF EXCIMER laser operating at 248 nm and delivering up to 8 MW in a 20 ns long pulse with a beam size of 1 cm x 2 cm. A telescope using cylindrical lenses reduces the size to 1 cm x 1 cm.

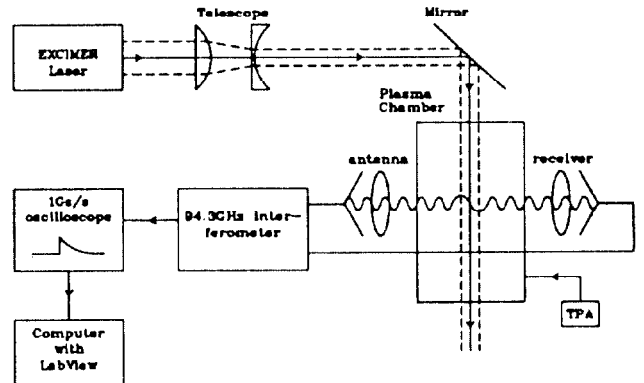


Figure 1: Lay-out of the plasma production experiment.

The plasma is diagnosed using 94.3 GHz microwave interferometry. The line averaged plasma density (no attenuation or refraction included) is given by

$$\bar{n} = \frac{\int_0^L n(x) dx}{L} = \frac{2\epsilon_0 mc}{e^2} \omega \frac{\Delta\phi}{L} \quad (7)$$

$$\text{or } \bar{n}[\text{cm}^{-3}] = 118.4 \frac{\omega/2\pi \Delta\phi[\text{rad}]}{L[\text{cm}]} \quad (8)$$

Here ω is the microwave frequency and $\Delta\phi$ is the change in phase seen by the microwave signal. The phase angle is obtained by first downconverting the launched and received signals to 500 MHz with a phase-locked 93.8 GHz Gunn oscillator and then mixing the 500 MHz signals in a double balanced mixer.

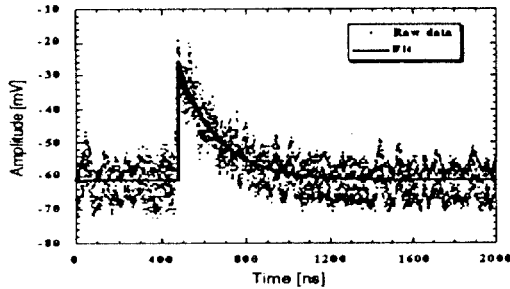


Figure 2: Typical interferometer result. The height of the signal is essentially proportional to the plasma density. Laser energy is 200 mJ and TPA pressure is 20 mTorr.

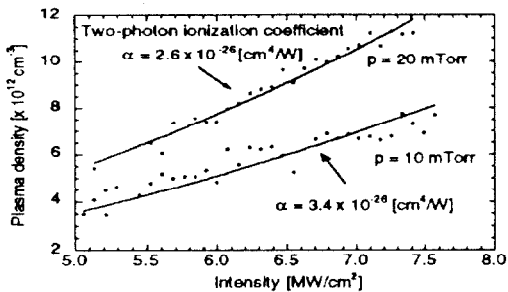
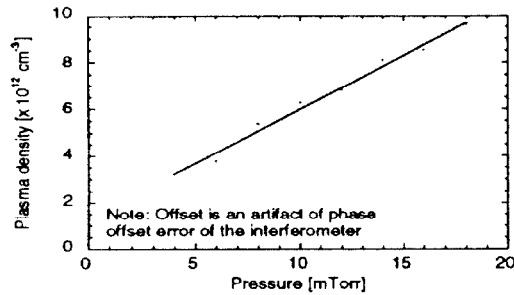


Figure 3 Plasma density vs. neutral filling pressure (linear dependence and intensity (quadratic dependence).

Typically the vacuum chamber is pumped down to about 7×10^{-6} Torr, isolated from the vacuum pump and back filled with the desired amount of TPA (10 mTorr up to 2 Torr). The microwave signal is launched transversely to the plasma column. The distance between launching and receiving horn is adjusted so that the double balanced mixer output is at a

minimum. Operating at this phase results in a better S/N performance but a slight loss in sensitivity for low plasma densities. A typical experimental data shot is shown in Fig. 2.

Using the interferometer we have experimentally verified the pressure and intensity scaling laws as predicted by the two-photon ionization model (Fig. 3). Using 20 mTorr of TPA and a laser energy of 200 mJ allows production of $1.3 \times 10^{13} \text{ cm}^{-3}$ plasma density with 10 % efficiency. The two-photon ionization coefficient is found to be about $3.0 \pm 0.4 \times 10^{-24} [\text{cm}^4/\text{W}]$ which is in reasonable agreement with the value $2.3 \times 10^{-24} [\text{cm}^4/\text{W}]$ obtained by Woodworth et al. [10].

Although the critical density n_c for 94.3 GHz radiation is about 10^{14} cm^{-3} , we have found experimentally that absorption limits the usefulness of the diagnostic to about $1/3 n_c$.

To overcome both the density limit and have spatial resolution, we are currently building a novel Fabry-Perot based optical interferometer. Design calculations indicate that the system will be capable of measuring plasma densities in the range of $10^{14} - 10^{16} \text{ cm}^{-3}$ with about $50 \mu\text{m}$ spatial resolution. Such a system will become essential for diagnosing plasma suitable for adiabatic focusing.

III. SUMMARY

A status report has been given on the upcoming 50 MeV plasma lens experiment at LBL. This experiment will be conducted at the BTF and will involve a systematic study of both over and underdense plasma lenses. Details of a parametric study of plasma production through two-photon ionization have been presented. The plasmas have been produced in a static fill of TPA using a KrF laser with intensities in the 5-10 MW/cm² range and have been diagnosed with a 94.3 GHz interferometer. Experimental and theoretical scaling laws for the plasma density are in overall agreement: linear with pressure, quadratic with intensity. Experiments on producing longitudinally tapered density profiles through the I² dependence on ionization yield are underway.

IV. ACKNOWLEDGMENTS

The authors wish to thank Glen Westenskow and Bob Stever from LLNL for lending the UV-laser system and the interferometer, respectively.

V. REFERENCES

- [1] P. Chen, Part. Accel. **20**, 171 (1987).
- [2] T. Katsouleas, "Optimal Density Taper for Plasma Lenses", USC, Dept. of Elec. Eng. Report 91-06-01 (1991).
- [3] P. Chen et al., Phys. Rev. Lett. **64**, 1231 (1990).
- [4] J. B. Rosenzweig et al., Phys. Fluids **B 2**, 1376 (1990).
- [5] H. Nakanishi et al., Phys. Rev. Lett. **66**, 1870 (1991).
- [6] G. Hairapetian et al., Phys. Rev. Lett. **72**, 2403 (1994).
- [7] W. Leemans et al., Proc. 1993 Part. Accel. Conf, 83 (1993).
- [8] M. de Loos et al., these proceedings.
- [9] W. Leemans et al., LBL-ESG Tech Note-199 (1992).
- [10] D. Whittum et al., Particle Accel. **34**, 89 (1990).
- [11] J. Woodworth et al., J. Appl. Phys. **57**, 1648 (1985).
- [12] J. Woodworth, private communication.